Storm intensity and old-growth forest disturbances in the Amazon region

F. D. B. Espírito-Santo,[1] M. Keller,[1,2,3] B. Braswell,[1,4] B. W. Nelson,[5] S. Frolking,[1] and G. Vicente[6]

Received 4 March 2010; revised 20 April 2010; accepted 29 April 2010; published 4 June 2010.

[1] We analyzed the pattern of large forest disturbances or blow-downs apparently caused by severe storms in a mostly unmanaged portion of the Brazilian Amazon using 27 Landsat images and daily precipitation estimates from NOAA satellite data. For each Landsat a spectral mixture analysis (SMA) was applied. Based on SMA, we detected and mapped 279 patches (from 5 ha to 2,223 ha) characteristic of blow-downs. A total of 21,931 ha of forest were disturbed. We found a strong correlation between occurrence of blow-downs and frequency of heavy rainfall (Spearman's rank, $r^2 = 0.84$, $p < 0.0003$). The recurrence intervals of large disturbances were estimated to be 90,000 yr for the eastern Amazon and 27,000 yr for the western Amazon. This suggests that weather patterns affect the frequency of large forest disturbances that may produce different rates of forest turnover in the eastern and western Amazon basin. **Citation:** Espírito-Santo, F. D. B., M. Keller, B. Braswell, B. W. Nelson, S. Frolking, and G. Vicente (2010), Storm intensity and old-growth forest disturbances in the Amazon region, *Geophys. Res. Lett.*, *37*, L11403, doi:10.1029/2010GL043146.

1. Introduction

[2] Are old-growth tropical forests in steady-state? Recent studies of permanent tree plots suggest that tropical forests are changing rapidly. Increases in the rate of turnover of trees and increasing carbon uptake (between 0.1 and 0.5 Mg C ha^{-1} y^{-1}) have been observed in permanent plots of neotropical and paleotropical forests [*Phillips and Gentry*, 1994]. There is accumulating evidence that old-growth tropical forests may be growing faster, experiencing changing patterns of recruitment and mortality [*Phillips and Gentry*, 1994], and increasing their stock of above-ground biomass [*Malhi et al.*, 2006].

[3] Local openings in the forest canopy (±100 m^2) are widely recognized as an important factor affecting the dynamics of tropical forests [*Hubbell et al.*, 1999]. Larger disturbances (≥1 ha) caused by cyclonic storms (hurricanes) also change the structure of tropical forests damaging hundreds of square kilometers [*Lugo et al.*, 1983]. In continental equatorial regions of the Amazon, hurricane damage does not occur. However, *Nelson et al.* [1994] used Landsat images of the Brazilian Amazon to detect large natural gaps (>30 ha) with fan-shape forms (blow-downs), probably caused by high-velocity wet downburst winds [*Garstang et al.*, 1998]. *Nelson et al.* [1994] identified 330 blow-downs in 137 Landsat TM between 1987 and 1989 of the Amazon, with a total disturbed area of 90,000 ha. The TM scene with the greatest total disturbance affected area had 16 blow-downs totaling 8,600 ha or 0.31% of the scenes. The largest single blow-down covered 3,370 ha, with the most frequent size classes falling between 30 and 100 ha. Most of these large blow-down areas (≥30 ha) occurred in the west-central basin of the Amazon, where annual precipitation is high.

[4] Forest damage by storms is most often associated with the intensity of wind gusts [*Lugo et al.*, 1983]. In the Amazon region wind gusts greater than 10 m s^{-1} accompanied by rainfall have been recorded [*Garstang et al.*, 1998]. Heavy rainfall caused by convective storms ought to correlate with strong winds and microbursts [*Fujita*, 1985]. In this study, we examine a regional mosaic of Landsat images and estimates of daily precipitation retrieved from satellite images to determine if there is a coherent spatial relation between heavy precipitation and large disturbances in old-growth forest in the Amazon. Earlier work [*Nelson et al.*, 1994; *Chambers et al.*, 2009] strongly suggests that severe convective storm activity associated with heavy rains causes intense winds that in turn lead to forest disturbance through blow-downs. We hypothesize that the weather patterns that cause blow-downs in the Amazon lead to different rates of forest turnover in the eastern and western Amazon basin.

2. Methods

2.1. Data and Study Area

[5] To evaluate the relation between severe storms and large disturbances in the Amazon, two regional data sets were integrated: (1) a multitemporal data set of Real-Time Rainfall (RTR) of the north continental area of South America, and (2) a mosaic of ETM+ Landsat images covering the precipitation gradient east to west across the Amazon basin from the east (2°13′S and 51°51′W) to west (6°29′S and 66°49′W).

2.2. Severe Storms in the Amazon Region

[6] The frequency of severe storms was determined by the integration of the RTR daily images produced by geosynchronous NOAA (National Oceanic and Atmospheric Administration) satellites [*Vicente et al.*, 1998]. RTR esti-

[1]Institute for the Study of Earth, Oceans and Space, University of New Hampshire, Durham, New Hampshire, USA.
[2]International Institute of Tropical Forestry, USDA Forest Service, Rio Piedras, Puerto Rico.
[3]NEON Inc., Boulder, Colorado, USA.
[4]Atmospheric and Environmental Research, Inc., Lexington, Massachusetts, USA.
[5]National Institute for Research in the Amazon, Manaus, Brazil.
[6]NESDIS, NOAA, Camp Springs, Maryland, USA.

0094-8276/10/2010GL043146

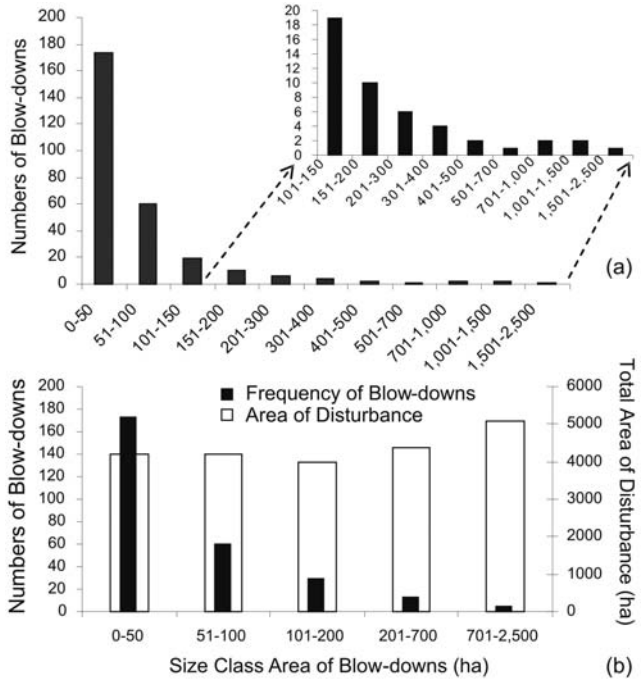

Figure 1. (a) Frequency distribution of the 279 classified blow-downs and (b) their corresponding disturbed areas classified in 27 Landsat images of an east-west transect of the Amazon.

mates are produced at 4 km spatial resolution using 10.7 mm band data from NOAA 8 satellites with adjustment for cloud top temperature gradients and moisture regimes using fields of precipitable water and relative humidity generated by the National Centers for Environmental Prediction ETA Model [*Vicente et al.*, 1998]. RTR daily images were obtained from 01 February to 31 December 1999. No data were obtained during January 1999 because of operational problems. We defined heavy rainfall as days with precipitation ≥20 mm d^{-1}.

2.3. Digital Classification of the Blow-Downs

[7] We have classified large disturbances as blow-downs based on spectral characteristics and spatial patterns identified previously [*Nelson et al.*, 1994; *Chambers et al.*, 2009] (see auxiliary material).[1] The number and area of large blow-downs in the Amazon were quantified using digital classification of 27 Landsat ETM+ images from 1999 to 2001 with low cloud cover (≤20%) and spatial resolution of ~28.5 m. All images were orthorectified with a spatial accuracy of ~15 m [*Tucker*, 2004]. A relative atmospheric correction was applied to the Landsat images using *Markham and Barker*'s [1987] algorithm.

[8] We applied a spectral mixture analysis (SMA) [*Shimabukuro and Smith*, 1991] in all six original ETM+ spectral bands to produce fraction images base on three end-members: green vegetation (GV), nonphotosynthetic vegetation (NPV) and shade (SD). Spectrally pure end-members were determined using the pure pixel index (PPI) [*Boardman et al.*, 1995].

[9] A semi-automated classification was applied to identify and to classify all blow-down events on the Landsat images. A pixel by pixel classification was developed using six bands (the GV, NPV and SD, plus the original bands 3, 4 and 5). The pixel groups were labeled using an unsupervised classification of Euclidean distance [*Schowengerdt*, 1997].

[10] We identified blow-downs when a cluster of more than 55 labeled pixels was observed in old growth forest with no sign of anthropogenic activity in the region. Clusters were generally fan-shaped [*Nelson et al.*, 1994]. Areas of anthropogenic disturbances (agriculture, pastures, secondary forests, roads and cities) or naturally exposed soils (patches of savanna shrubs and trees, savanna herbs, open vegetation on white sand and dry river borders) were excluded from our analysis (see auxiliary material). The blow-downs were also classified into two age classes (old > 2 y and new < 2 y) according to the relative proportions of GV and NPV (see auxiliary material for more details).

2.4. Spatial Point Patterns of Blow-Downs

[11] Were large disturbances clustered spatially? To observe if the blow-downs exhibited any systematic spatial pattern distribution, a spatial point analysis (SPA) was carried out [*Ripley*, 1981]. A SPA consists of a set of points (s_1, s_2, etc.) in a defined study region (R) divided into sub-regions ($A \subseteq R$). $Y(A)$ is the number of events that occurred in sub-region A. In a spatial context, the number of points can be estimated by use of their expected value E ($Y(A)$), and covariance COV ($Y(A_i)$, $Y(A_j)$), given that Y is the event number in areas A_i and A_j. The intensity of an event $\lambda(s)$ is the frequency of points of a specific location s, where ds is the area of this region. The intensity of events or in our case, blow-downs, can be represented as:

$$\lambda(s) = \lim_{ds \to 0} \left\{ \frac{E(Y(ds))}{ds} \right\} \quad (1)$$

Because SPA only requires the spatial location of each event, we calculated the centroid of each classified blow-down. Next, we used a Gaussian smoothing algorithm named kernel with a tested bandwidth of 50 km to produce the spatial clusters of blow-downs and a probability density function k [*Ripley*, 1981] to examine the spatial dependence of these events (see auxiliary materials).

2.5. Recurrence Intervals of Blow-Downs

[12] We used the following assumptions to calculate the recurrence intervals of the large disturbances detected in the Amazon: (i) only new blow-downs up to 2 years old were used to calculate the recurrence time, considering that probability of detection decreases with age of the regrowth in older patches; and (ii) disturbances occurred at a constant rate during the two years of detection. The recurrence interval (T) was calculated as:

$$T = \frac{A_{forest}}{D_{AR}}, \quad \text{where } D_{AR} \text{ is:} \quad (2)$$

$$D_{AR} = \frac{A_{new-blowdown}}{Y} \quad (3)$$

[1] Auxiliary materials are available in the HTML. doi:10.1029/2010GL043146.

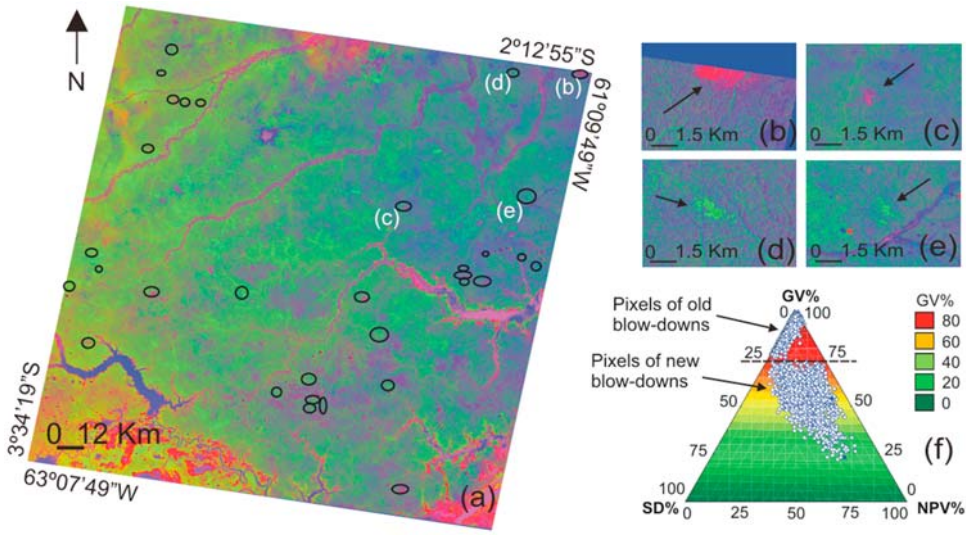

Figure 2. (a) Unmixing Landsat image in color composition NPV (R), GV (G) and SD (B) showing the spatial distribution of several blow-downs. Close-up view of (b and c) new blow-downs with probable age <2 yrs and (d and e) old blow-downs likely >2 yrs old. (f) General fraction image proportions of new (n = 3539 pixels) and old blow-downs (n = 1869 pixels), sampled from the correspondent unmixed Landsat image (Figure 2a). Vertices of the ternary diagram (clockwise from top) represent 100% of GV, NPV and SD fraction images.

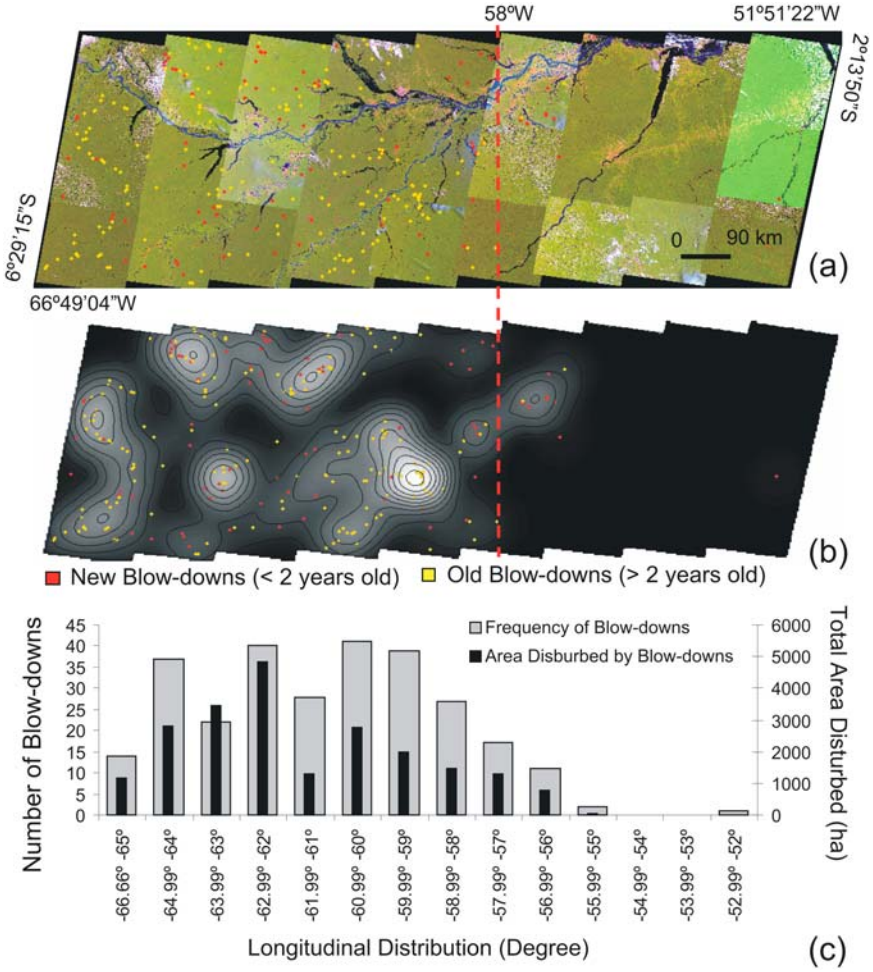

Figure 3. (a) Spatial distribution of the 279 blow-down disturbances >5 ha and (b) their spatial clustering observed in the east-west image transect of the Amazon. (c) East-west distribution of blow-down frequency and area.

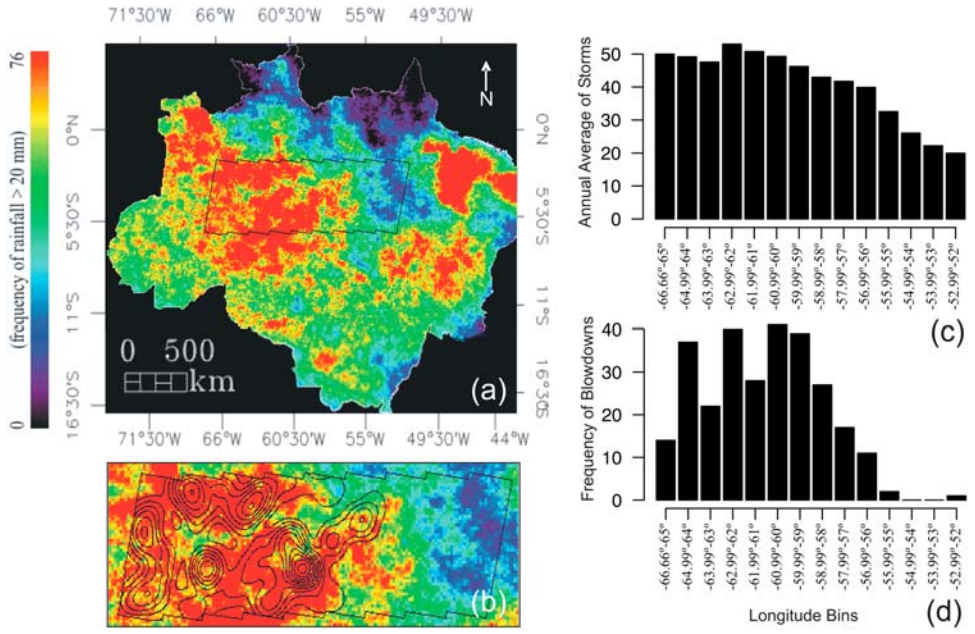

Figure 4. (a) Annual frequency of intense storms in the Amazon (number of days with >20 mm of rain) produced by 313 RTR daily images of the year 1999. (b) Clusters of large disturbances coincide with areas of more high-intensity storms. Frequency of the annual average of (c) storms and (d) blow-downs taken from one degree of longitude bins.

where A_{forest} is the total area of forest and D_{AR} is the disturbance rate. D_{AR} is estimated from the total area of new blow-downs ($A_{blow\text{-}down}$) during the time interval Y (maximum interval of detection equal to 2 years). Thus, the recurrence interval can be rewritten as:

$$T = \frac{A_{forest}}{(A_{new-blowdown}/2)} = 2\left(\frac{A_{forest}}{A_{new-blowdown}}\right) \quad (4)$$

3. Results

3.1. Size Class Distribution and Unmixing Spectral Properties of Blow-Downs

[13] In 27 Landsat images, we mapped 279 patches as large disturbances that we refer to as blow-downs accounting for a total of 21,931 ha. Of that area, 17,822 ha (189 patches) were old blow-downs (>2 years old), and 4,109 ha (90 patches) were recent blow-downs. The largest blow-down covered 2,223 contiguous hectares. The smallest blow-down observed was 5 ha based on the minimum threshold of blow-down detection of ~55 pixels. Blow-downs smaller than 50 ha were most frequent (Figure 1a). Blow-downs greater than 101 ha, although rare, accounted for 61.6% of total blow-down disturbance area of this region (Figure 1b).

[14] Based on the unmixing spectral proprieties of each Landsat image (Figure 2a) new blow-downs (Figures 2b and 2c) had on average 28% of NPV (±10.20% sd), 54% of GV (±9.53% sd) and 17% of SD (±6.20% sd) (Figure 2f). Old blow-downs (Figures 2d and 2e) had 1% of NPV (±1.34% sd), 94% of GV (±5.46% sd) and 5% of SD (±4.75% sd) (Figure 2f).

3.2. East-West Distribution of Disturbances and Severe Storms

[15] The occurrence of blow-downs (≥5 ha) over the Amazon region investigated is not uniform. Most occurred between 58°00′W and 66°49′W (Figure 3a). Several clusters of blow-downs were detected in the western Amazon (Figure 3b). Blow-downs were infrequent in the eastern basin (51°51′W to 58°00′W). The greatest area disturbed by blow-downs occurred between the longitudes 62° and 63.99°, where ~5,000 ha of old growth forest were disturbed by 40 large blow-downs (Figure 3c). Old and new blow-downs had similar spatial distributions (Figures 3a and 3b).

Table 1. Frequency, Disturbed Area and Recurrence Interval of Blow-Downs[a]

Domain	Landsat Scenes	Forest (km^2)	All Blow-Downs			New Blow-Downs			T[c] (yr (10^3))
			Numbers	km^2	Proportion[b]	Numbers	km^2	Proportion[b]	
Full	27	793076	279	219	0.0277%	90	41.1	0.0052%	39
Eastern[d]	12	339579	21	18.5	0.0054%	13	7.51	0.0022%	90
Western[d]	15	453497	258	201	0.0443%	77	33.6	0.0074%	27

[a]Recurrence interval: T, in years.
[b]Proportion is (blow-down area ÷ by total area of forest) × 100%.
[c]Assumes a constant disturbance rate and detectability of 2 years T = forest area ÷ (new blow-down area ÷ detectability interval). See section 2.5.
[d]Eastern domain: 51°51′22″W to 57°25′18″W; Western domain: 57°25′18″W to 66°49′04″W.

[16] We provide a quantitative linkage between blow-down occurrence and the frequency of heavy daily rainfall in the Amazon region associated with severe convective activity [*Garstang et al.*, 1998]. Blow-down occurrence frequency and the associated disturbance area were greater where severe storms occurred more frequently (Figures 4a and 4b). The relation between rainfall (Figure 4c) and frequency of blow-downs (Figure 4d), although nonlinear, (see auxiliary material) has a strong and significant correlation (Spearman's rank, $r^2 = 0.84$, $p < 0.0003$).

[17] A comparison of the eastern and western portions of our study region (Figure 3) shows a strong contrast in the blow-down recurrence intervals. Based on the occurrence of new blow-downs and the assumption of a constant disturbance rate (section 2.5), we estimated the recurrence interval for blow-downs in the eastern region is 90,000 yr while it is only 27,000 yr for the western region (Table 1).

4. Discussion

[18] We confirm the conclusions of the earlier study by *Nelson et al.* [1994] and expand on their work by using semi-automatic digital classification for detection and mapping of blow-downs in the Amazon and a satellite proxy measurement for convective storm events. In the study by *Nelson et al.* [1994], the threshold minimum area of disturbance was 30 ha. By using spectral unmixing and pixel by pixel classification of Landsat images we reduced the threshold of detection for blow-downs to about 5 ha (~55 pixels). Both studies found that new plus old blow-down disturbances represented a small fraction of the entire studied area of undisturbed forests (~0.02%). Through digital processing, we were able to not only improve the spatial resolution but also improve the temporal resolution with important implications that we discuss below.

[19] The frequency distribution of storms and frequency of blow-downs suggest a nonlinear relationship, which is not entirely surprising, considering that cloud-top temperature is only a proxy of storm severity, and considering the spatial and temporal mismatches between recorded blow-downs and the RTR data set. The RTR rainfall data set used provides increased spatial resolution (4 km) and higher frequency compared to earlier climatologies to isolate the importance of severe storm events. Closer linkage of blow-down events to storm conditions will require high-frequency observations of rainfall (now available) and high-frequency ground-based records of disturbance over wide areas (currently unavailable).

[20] Although the disturbance rates are certainly higher in western Amazon, the estimate of recurrence interval for blow-downs remains highly uncertain. Estimating a millennial-scale recurrence interval from two years of observations (the period of detection), depends on the assumption that disturbance rates during those two years are representative of this disturbance process over millennia. Nonetheless, the east-west asymmetry in the frequency distribution of blow-downs is consistent with the geographic distribution of disturbance-adapted tree genera [*ter Steege et al.*, 2006], suggesting that, over the long-term, disturbance events are less frequent in eastern compared to western Amazon. However, long-term changes of climate [*Mayle and Power*, 2008] and patterns of soil fertility [*Malhi et al.*, 2006] and geology [*Rossetti et al.*, 2005] would be much more important environmental factors affecting the distribution of plant species and plant functional types.

[21] Assuming that the blow-down damages all the trees and considering the average range of biomass for the Amazon is between 150 and 350 Mg ha^{-1} [*Houghton et al.*, 2000], we estimate that carbon emission caused by blow-down mortality (area of blow-downs × range of mean biomass) would contribute at most only 0.3 to 2 Tg C y^{-1} for the 27 Landsat images analyzed, although, it will be compensated by the regrowth of secondary forests. Given that net deforestation releases between 200 and 300 Tg C y^{-1} [*Houghton et al.*, 2000] in the Amazon, blow-down disturbance events do not make an important direct contribution to carbon dioxide emissions or even for the overall forest succession process in the tropics. While the contemporary effect of large blow-downs is small with regard to carbon and nutrient cycling, our study raises the question of the possible importance of convective storm activity as a control over the rate of forest disturbance in general across the Amazon. If convective activity is also responsible for smaller scale disturbances also, this process may help explain some of the asymmetry in tree mortality and turnover rates found for the Eastern and Western areas of the Amazon forest [*Phillips and Gentry*, 1994].

[22] **Acknowledgments.** This research was supported by the NASA Earth System Science Fellowship (NESSF) (grant NNX07AN84N) and the NASA Terrestrial Ecology Program contribution to the Large Scale Biosphere-Atmosphere Experiment in the Amazon (LBA).

References

Boardman, J. W., F. A. Kruse, and R. O. Green (1995), Mapping target signatures via partial unmixing of AVIRIS data, paper presented at the Fifth Annual JPL Airborne Workshop, Jet Propul. Lab., Pasadena, Calif.

Chambers, J. Q., A. Robertson, V. Carneiro, A. Lima, M.-L. Smith, L. Plourde, and N. Higuchi (2009), Hyperspectral remote detection of niche partitioning among canopy trees driven by blowdown gap disturbances in the central Amazon, *Oecologia*, *160*, 107–117, doi:10.1007/s00442-008-1274-9.

Fujita, T. T. (1985), The Downburst: Microburst and Macroburst, Satellite and Mesometeorology Research Project (SMRP), report, Univ. of Chicago, Chicago, Ill.

Garstang, M., S. White, H. H. Shugart, and J. Halverson (1998), Convective cloud downdrafts as the cause of large blowdowns in the Amazon rainforest, *Meteorol. Atmos. Phys.*, *67*, 199–212, doi:10.1007/BF01277510.

Houghton, R. A., D. L. Skole, C. A. Nobre, J. L. Hackler, K. T. Lawrence, and W. H. Chomentowski (2000), Annual fluxes of carbon from deforestation and regrowth in the Brazilian Amazon, *Nature*, *403*, 301–304, doi:10.1038/35002062.

Hubbell, S. P., R. B. Foster, S. T. O'Brien, K. E. Harms, R. Condit, B. Wechsler, S. J. Wright, and S. Loo de Lao (1999), Light-Gap disturbances, recruitment limitation, and tree diversity in a neotropical forest, *Science*, *283*, 554–557, doi:10.1126/science.283.5401.554.

Lugo, A. E., M. Applefield, D. J. Pool, and R. B. McDonald (1983), The impact of Hurricane David on the forests of Dominica, *Can. J. For. Res.*, *13*, 201–211, doi:10.1139/x83-029.

Malhi, Y., et al. (2006), The regional variation of aboveground live biomass in old-growth Amazonian forests, *Global Change Biol.*, *12*, 1107–1138, doi:10.1111/j.1365-2486.2006.01120.x.

Markham, B. L., and J. L. Barker (1987), Radiometric properties of U.S. processed Landsat MSS data, *Remote Sens. Environ.*, *22*, 39–71, doi:10.1016/0034-4257(87)90027-7.

Mayle, F. E., and M. J. Power (2008), Impact of a drier early-mid-Holocene climate upon Amazonian forests, *Philos. Trans. R. Soc. B.*, *363*, 1829–1838, doi:10.1098/rstb.2007.0019.

Nelson, B. W., V. Kapos, J. B. Adams, W. J. Oliveira, O. P. G. Braun, and I. L. Amaral (1994), Forest disturbance by large blowdowns in the Brazilian Amazon, *Ecology*, *75*, 853–858, doi:10.2307/1941742.

Phillips, O. L., and A. H. Gentry (1994), Increasing turnover through time in tropical forests, *Science*, *263*, 954–958, doi:10.1126/science.263.5149.954.

Ripley, B. D. (1981), *Spatial Statistics*, 132 pp., John Wiley, New York.

Rossetti, D. D., P. M. de Toledo, and A. M. Goes (2005), New geological framework for Western Amazonia (Brazil) and implications for biogeography and evolution, *Quat. Res.*, *63*, 78–89, doi:10.1016/j.yqres.2004.10.001.

Schowengerdt, R. A. (1997), *Remote Sensing: Models and Methods for Image Processing*, 522 pp., Academic, San Diego, Calif.

Shimabukuro, Y. E., and J. A. Smith (1991), The least-squares mixing models to generate fraction images derived from remote sensing multispectral data, *IEEE Trans. Geosci. Remote Sens.*, *29*, 16–20, doi:10.1109/36.103288.

ter Steege, H., et al. (2006), Continental-scale patterns of canopy tree composition and function across Amazonia, *Nature*, *443*, 444–447, doi:10.1038/nature05134.

Tucker, J. (2004), G. D. M., and J. D. Dykstra, NASA's global orthorectified Landsat data set, *Photogram. Eng. Remote Sens.*, *70*, 313–322.

Vicente, G. A., R. A. Scofield, and W. P. Menzel (1998), The operational GOES infrared rainfall estimation technique, *Bull. Am. Meteorol. Soc.*, *79*, 1883–1898, doi:10.1175/1520-0477(1998)079<1883:TOGIRE>2.0.CO;2.

B. Braswell, F. D. B. Espírito-Santo, and S. Frolking, Institute for the Study of Earth, Oceans and Space, University of New Hampshire, 8 College Rd., Room 481, Durham, NH 03824, USA. (f.delbon@gmail.com)

M. Keller, NEON Inc., 5340 Airport Blvd., Boulder, CO 80301, USA.

B. W. Nelson, National Institute for Research in the Amazon, Av. André Araújo, 2936, Manaus, CEP 69060-001, Brazil.

G. Vicente, NESDIS, NOAA, 5200 Auth Rd., Camp Springs, MD 20746, USA.